

Graphene Multi-Protonation: a Cooperative Mechanism for Proton Permeation

Massimiliano Bartolomei ^{*}, Marta I. Hernández, and José Campos-Martínez

Instituto de Física Fundamental, Consejo Superior de Investigaciones Científicas (IFF-CSIC), Serrano 123, 28006 Madrid, Spain

Ramón Hernández Lamonedá

Centro de Investigaciones Químicas, Universidad Autónoma del Estado de Morelos, 62210 Cuernavaca, Mor. México

(Dated: January 10, 2019)

The interaction between protons and graphene is attracting a large interest due to recent experiments showing that these charged species permeate through the 2D material following a low barrier (~ 0.8 eV) activated process. A possible explanation involves the flipping of a chemisorbed proton (rotation of the C-H⁺ bond from one to the other side of the carbon layer) and previous studies have found so far that the energy barriers (around 3.5 eV) are too high to explain the experimental findings. Contrarily to the previously adopted model assuming an isolated proton, in this work we consider protonated graphene at high local coverage and explore the role played by nearby chemisorbed protons in the permeation process. By means of density functional theory calculations exploiting large molecular prototypes for graphene it is found that, when various protons are adsorbed on the same carbon hexagonal ring, the permeation barrier can be reduced down to 1.0 eV. The related mechanism is described in detail and could shed a new light on the interpretation of the experimental observations for proton permeation through graphene.

PACS numbers:

^{*} Corresponding author, e-mail: maxbart@iff.csic.es

1. INTRODUCTION

This work is partly motivated by recent experimental work on the permeation at room temperature of protons through graphene[1]. In that study, Geim and coworkers reported conductance and mass spectroscopy measurements of proton transport through pristine graphene and found that, in a temperature range of 270-330 K, the process exhibits an Arrhenius-type behavior with a rather low activation energy (about 0.8 eV). Moreover, protons permeate through this two-dimensional crystal about ten times faster than deuterons[2]. These discoveries were absolutely unexpected since graphene was believed to be completely impermeable to all atoms and molecules under ambient conditions[3, 4]. A number of works have subsequently appeared -both experimental[5–10] and theoretical[11–16]- not only stimulated by the promise of important applications in hydrogen technology but also with the aim to uncover the microscopic mechanisms underlying these observations.

Despite much recent progress on the theoretical insight into the processes leading to such a facile permeation of protons through graphene [11–16], we consider that a complete and satisfactory understanding has not been achieved yet (e.g. see Refs.[11, 12] for some discussions). The possible role of surface defects in the transport process[5, 6] has been also indicated. Some works[15, 16] have emphasized the role of quantum tunneling in effectively lowering the energy barrier and on isotope selectivity, using models that assume that protons/deuterons are free particles. In the experiments, however, protons are initially moving within an aqueous medium (hydrated Nafion or HCl solution), so other works[12–14] have more realistically considered protons to be bound to water (as H_3O^+) in the reactants states. As Shi et al[12] indicate, two possible modes for the penetration of a hydrated proton can be distinguished. The first one (dissociation-penetration) involves the removal of the proton from the water network as it crosses the graphene membrane through the hollow of a carbon ring. It has been found that this mechanism is unlikely due to the large proton affinity of water[12, 13]. Interestingly, Feng *et al*[14] have recently found, by means of first principles calculations, that the proton transport can be largely facilitated if various carbon atoms of the graphene layer (close to the crossing region) are in sp^3 configurations due to hydrogenation. In the second mechanism (adsorption-penetration), a proton is transferred from the aqueous media to the graphene surface, where it becomes chemisorbed at the top of a carbon atom and, in a second step, it flips through the hollow from the original chemisorbed site

to a related one on the other side of the layer. Previous works[14] indicate that the barrier for proton transfer from water to a chemisorbed state is small and therefore the first step appears to be feasible at ambient conditions. However, the chemisorbed state is very stable, hence the barrier for the proton flipping becomes extremely high (~ 3.5 eV[4, 11, 14]).

In this work, we assume that the chemisorbed proton is not initially isolated but surrounded by a number of protons that are chemisorbed as well and, in this way, we aim to explore the role of these neighbors on the flipping process. In other words, it is supposed that protons have been already transferred from the water network to a set of chemisorption sites so that the graphene sheet becomes partially protonated on one of its sides. It is found that, if two protons respectively attach to two consecutive carbon atoms, the permeation mechanism is completely different to that of an isolated chemisorbed proton. First, the energy barrier drops quite significantly (down to about 1.0 eV). Second, in contrast with the isolated case, where the reaction path goes through a planar transition state near the center of the carbon ring, the path for the multiprotonated case involves the insertion of the flipping proton into the middle of an effectively broken C-C bond. This bond is restored once the flipping process comes to an end, therefore preserving the stability of the carbon layer. These findings can help to rationalize the proton permeation observations[1]; additionally, they could provide some clues about properties of hydrogenated graphene[17, 18] or about astrochemical processes involving hydrogen/protons and carbonaceous surfaces[19, 20].

The mechanism here investigated bears some resemblance with that proposed in a study by Lee *et al*[21] on the electrochemical storage of hydrogen within a narrow single-walled carbon nanotube (SWCNT), where a low energy reaction path was identified for a hydrogen atom flipping from the external to the internal side of the nanotube. In addition, it is also worth noting that our study apparently shows similarities with that of Feng *et al*[14], in the sense that in both cases it is concluded that the barrier for proton penetration notably decreases upon local protonation/hydrogenation. However, the involved microscopic mechanisms are completely different. A detailed comparison with the above mentioned works is provided at the end of Section 3.

The paper is organized as follows. Computational methods are described in the following section. Next, results are presented and discussed, starting with an analysis of the stability of protonated graphene and continuing with a study of the permeation process as a function of the number of chemisorbed protons along a carbon ring. The report closes with a summary

where further lines for research are indicated.

2. COMPUTATIONAL METHODS

We have carried out electronic structure calculations to study the role played by an increasing number of protons ($n = 1 - 6$), all chemisorbed along a given carbon ring of graphene, in their penetration through the 2D layer, which have been described exploiting a molecular model. In previous works the coronene molecule was found to be a sufficiently accurate model for the study of the physical adsorption of single atoms[22, 23] or the sticking of hydrogen atoms[24, 25] to graphene. Here, a larger molecular prototype is required to correctly describe a more complex process involving a larger number of adsorbed species and, to this end, we have found that the use of circumcoronene ($C_{54}H_{18}$) is sufficiently adequate for the present purposes. A significant advantage of using molecular prototypes is that an arbitrary number of protons can be included in the calculation, whereas periodic calculations suffer from the problem of having to neutralize the unit cell to converge and this procedure becomes less reliable when increasing the number of charges.

DFT calculations have been performed for the optimization of the protonated circumcoronene structures by using the PBE[26] functional together with the cc-pVTZ[27] basis set. These calculations were found to be in good agreement with benchmark MP2/aug-cc-pVTZ computations carried out for a smaller carbon plane prototype such as coronene. Additional calculations involving larger prototypes ($C_{96}H_{24}$ and $C_{150}H_{30}$) were carried out with a reduced 6-311+G[28] basis set. We have verified that, in the case of circumcoronene, this smaller set provides energy variations that are in good agreement (within few percents) with those obtained with the cc-pVTZ[27] basis set. All reported energies correspond to stationary points whose correct nature has been verified by carrying out harmonic frequency calculations, used in turn to estimate zero-point energy and thermal corrections (at 298 K and 1 atm) to thermodynamic properties. The enthalpy of the proton in the gas phase have been estimated to be $\frac{5}{2}RT$ as a result of the application of the standard statistical mechanics and ideal gas expressions. Intrinsic reaction coordinate calculations have been employed to check that reactants and products are indeed connected with the transition states for various of the permeation processes.

All DFT computations have been performed by using the Gaussian 09 code[29].

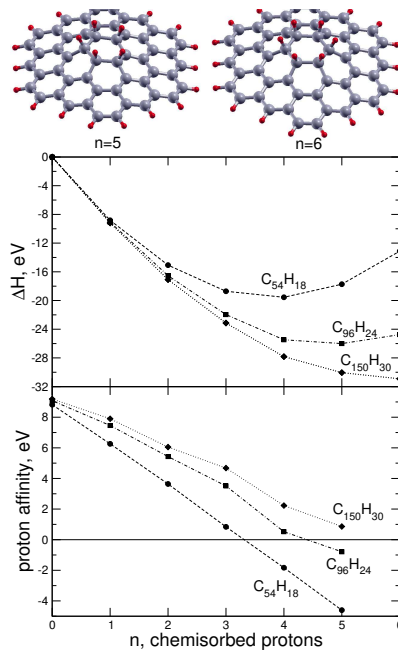
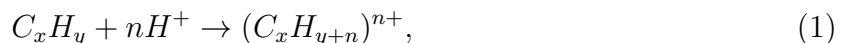


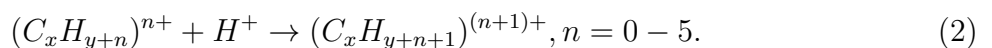
FIG. 1: Sequential protonation of a graphenic single ring. Upper panel: corresponding enthalpy variation with respect to the unprotonated graphene molecular prototype ($n=0$) and isolated protons. Lower panel: proton affinity of each protonated graphene prototype ($(C_x H_{y+n})^{n+}$, $n=0-5$). The dashed, solid and dotted lines correspond to the $C_{54}H_{18}$ (circumcoronene), $C_{96}H_{24}$ (circumcircumcoronene) and $C_{150}H_{30}$ (circumcircumcircumcoronene) prototypes, respectively.

3. RESULTS AND DISCUSSION

First, we address the question of graphene affinity for the chemical adsorption of protons. Structures of circumcoronene for the sequential sticking of protons above its central ring are illustrated in Fig. 1. In the upper panel of Fig. 1, we report the enthalpy variation (ΔH) as a function of the number n of chemisorbed protons, which corresponds to the gas phase process



where $C_x H_y$ represents the unprotonated ($n=0$) graphene prototype. In the lower panel we depict instead the proton affinity of each protonated graphene prototype, which is defined as $-\Delta H$ of the following process



It can be seen that in the case of circumcoronene ($C_{54}H_{18}$) the consecutive addition of a proton to the inner ring is an energetically favourable process: in fact, positive proton affinities are obtained for n up to 3, that is up to four protons could be adsorbed. A similar result was previously theoretically described[30] for the multiprotonation of benzene, for which the addition of up to 3 protons was found to lead to stable molecular structures, that is preserving the hexagonal ring. In this case, it seems also clear that the stability of the most protonated ($n=5,6$) fragments depends on the size of the considered graphene flakes. In fact, when larger graphene molecular prototypes ($C_{96}H_{24}$ and $C_{150}H_{30}$) are taken into account we observe (upper panel of Fig. 1) progressively larger enthalpy variations which seem to tend towards a converged profile as a function of n . In particular, in the case of the circumcircumcircumcoronene ($C_{150}H_{30}$) prototypes, positive proton affinities are found for all considered protonated fragments, that is the chemisorption of up to 6 protons is feasible and leads to stable molecular structures. These results suggest that the saturation of a graphenic ring with protons is energetically possible in the gas phase and we can expect even more favorable proton affinities for larger graphene flakes.

It is also crucial for the adopted model to mention that the local properties of the multi-protonated site are found to barely depend on the size of the graphene flake. For example, partial charges and bond distances of the central ring of a 6 times protonated circumcoronene are very similar to those of an analogously protonated circumcircumcoronene. Note that the net charge of this central ring is about +0.5 so that an excess charge of about +5.5 spreads over the rest of the flake. It is reasonable that this excess charge becomes more easily distributed as the size of the prototype increases, hence this feature must be at the origin of the larger proton affinities of the bigger prototypes (Fig. 1). In addition, we have also noticed that, once the C-H⁺ bond is formed, most of the proton character is lost as the partial charge on hydrogen is very close (slightly larger) to that typical of an usual C-H bond. Nevertheless, to remind the reader that the whole graphene flakes have the charge of the added protons, the positive charge on the hydrogen atoms will be retained in the notations used below.

Having established the stability of the graphene prototypes when several protons are chemisorbed on a benzenic ring, we start studying the permeation process for one and two chemisorbed protons as well as the underlying microscopic mechanism. In Fig. 2, the proton penetration from one side to the other of the carbon plane is considered for the case of a single

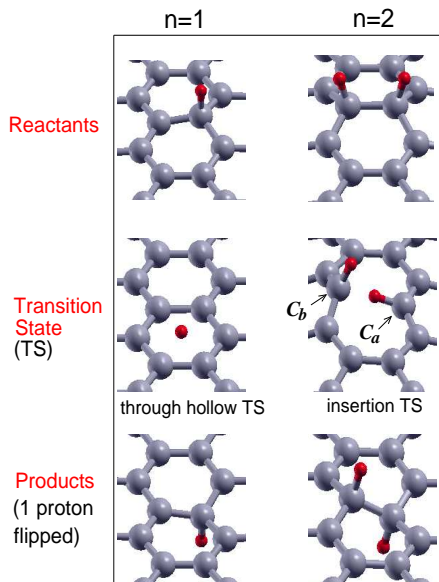


FIG. 2: Most favorable proton flipping mechanisms for the consecutive protonation (up to two protons) of a graphenic single ring. The first row shows the reactants configuration with adjacent protons chemisorbed on the same side of the carbon plane. The second row shows the transition state (TS) configuration. For $n=2$, carbon atoms bound to the flipping proton and to the adjacent proton are indicated as C_a and C_b , respectively. The last row shows the products configuration with one proton flipped on the other side of the carbon plane. The corresponding electronic energy and enthalpy balances are reported in Table I.

chemisorbed proton ($n = 1$) as well as for that of two protons attached to two consecutive carbon atoms ($n = 2$). For the isolated proton the transition state (TS) corresponds to a planar structure: the $C-H^+$ bond rotates to locate the proton near the center of the ring (termed as “hollow” TS) and continues the rotation to end up in an equivalent chemisorption state at the other side. Notice that at the TS the original $C-H^+$ bond has been broken. However, as pointed out by Miao and coworkers[4], there are chemical interactions of the proton with the surrounding carbon atoms in the ring. Still, the corresponding activation energy (ΔE_a) is quite high and close to 3.5 eV as reported in Table I. Similar results have

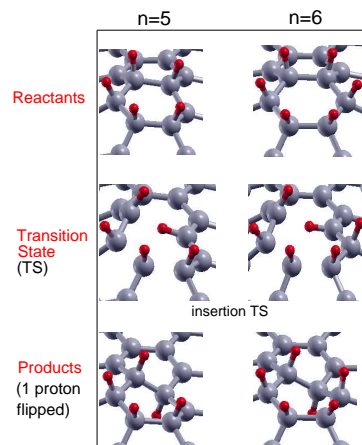


FIG. 3: As in Fig. 2 but with five and six protons chemisorbed on the graphenic single ring.

already been obtained from previous calculations at the DFT level[4, 11, 14]. However, for two nearby chemisorbed protons the most favourable reaction path is quite different: the related TS is not planar and we observe the insertion of the proton through the middle of the C-C bond connecting to the closest chemisorbed additional proton (“insertion” TS). For this to occur, the length of that C-C bond changes from 1.55 (reactants) to 2.39 Å (TS), so the bond effectively breaks. Interestingly, this breaking of the C-C bond does not provoke a large energetic penalty as could be expected. On the contrary, as shown in Table I, the corresponding activation energy is about 2.8 eV, lower than that of the single chemisorbed proton. In part this is due to the fact that, during the insertion, the C-H⁺ bond is preserved as opposed to the $n = 1$ case where such a bond is broken.

To get insight into this new mechanism, we have examined in detail the structures of the corresponding stationary points (right panel of Fig. 2). Let us denote H_a⁺ and H_b⁺ as the flipping and adjacent protons, respectively, and C_a and C_b, as the carbon atoms linked to those protons (see right central panel of Fig. 2). Initially, these carbon atoms exhibit four bonds in a sp³-like hybridization (i.e., C_a is bound to H_a⁺, to C_b and to two other adjacent

TABLE I: Electronic energy and enthalpy variations associated to the most favorable single proton flipping process for an increasing number (n) of adjacent chemisorbed protons on a graphenic carbon ring. The cases of $n=1,2,5$ and 6 are illustrated in Figs. 2 and 3. The first two columns show the energy balances between reactants (R) and transition state (TS) while the last columns, those between reactants and products (P). The last line reports the values for the arrangement of five protons on a ring plus one proton on a surrounding ring (Fig. 5), leading to the lowest activation energy. Values are in eV.

chemisorbed protons	R→TS		R→P	
	ΔE_a	ΔH_a	ΔE_r	ΔH_r
n=1	3.44	3.24	0.00	0.00
n=2	2.77	2.65	-0.39	-0.39
n=3	2.29	2.17	-0.38	-0.42
n=4	1.76	1.69	-0.37	-0.37
n=5	1.53	1.44	-0.46	-0.47
n=6	1.61	1.50	-1.21	-1.20
n=5+1	1.01	0.95	-0.55	-0.56

carbon atoms of the graphenic network, the corresponding C-C distances, 1.50-1.55 Å, being typical of single bonds). At the TS, the C_a - C_b bond is broken but the C_a atom keeps its bonding with the three remaining atoms, showing, however, quite different bond distances and angles (C-C distances are reduced to 1.36 Å). Indeed, these four atoms nearly exhibit a planar geometry (with $C - \widehat{C}_a - H_a^+$ and $C - \widehat{C}_a - C$ angles of 113° and 134° , respectively), indicating that the C_a atom approximately adopts a sp^2 configuration. Analogously, the three remaining bonds around the C_b atom have transformed towards a trigonal planar geometry (angles $C - \widehat{C}_b - H_b^+$ and $C - \widehat{C}_b - C$ being 118.5° and 122° , respectively), thus showing also C_b a sp^2 configuration. Although the distance between the flipping proton and the opposite carbon atom at the TS, $H_a^+ - C_b$, is short (1.32 Å) it does not correspond to a bonding interaction but rather to a repulsive one. This is to be expected considering that, as stated before, the proton character in the $C_a H_a^+$ bond has been mostly lost and therefore it can only experience a steric repulsion with the C_b atom. This will be further confirmed

below as a correlation between the $H_a^+-C_b$ distances and the barrier heights. Given that a C-C bond has been broken it is natural to enquire whether an open-shell structure with unpaired electrons characterizes the TS. We have performed stability tests of the closed-shell PBE determinant which prove it is stable and corresponding to the lowest energy solution (from the comparison with triplet states and unrestricted solutions). Therefore, as a qualitative explanation for the relatively low activation energy of this insertion process, it can be said that the cost of breaking the C-C bond at the TS is compensated by the transformation of the remaining bonds to stronger sp^2 -type ones. We have checked that, when additional adsorbed protons are added to the same ring of carbon atoms, the penetration process most favourably occurs through the same kind of insertion TS, as can be seen, for instance, in Fig. 3 for the case of five and six protons.

Additional adsorbed protons have been consecutively added along the central ring of the circumcoronene molecule and the results for the proton permeation are collected in Table I and in Fig. 4. Note that the flipping proton is that located at one end of the row of chemisorbed protons, as indicated schematically in the upper part of Fig. 4. It is found that the activation energy further decreases with the protonation degree, reaching a minimum of $\Delta E_a=1.53$ eV for $n = 5$ (less than half of the value for $n=1$) and then slightly increasing to 1.61 eV for $n = 6$. The corresponding enthalpies are roughly 0.10 eV smaller than the activation energies, in accordance with the finding that the zero point energy is larger for reactants than for the TS. On the other hand, as seen in Fig. 4 (middle panel), the C_a-C_b distance in the reactants state monotonously increases with n up to $n = 5$. This is a consequence of the amplification of the ring area, in turn due to the increasing number of single C-C bonds and effects of steric repulsion between hydrogens. This feature probably facilitates a larger C_a-C_b distance in the TS (as indeed seen in the lower panel of Fig. 4) and therefore an easier insertion of the proton between the two carbon atoms (a lower energy barrier). In fact, the $C_b-H_a^+$ distance increases from 1.32 Å for $n =2$ to 1.52 Å for $n =6$ whereas the $C_a-H_a^+$ distance stays in the range of 1.07-1.08 Å in the whole n range studied.

From Table I it can also be seen that (except for $n=1$ where initial and final states are equivalent) the flipping process is exothermic with electronic energy and enthalpy variations (ΔE_r and ΔH_r) ranging between -0.4 to -0.5 eV for $n=2-5$. This result is not surprising since in related systems as hydrogenated graphene[31] the most stable states involve adjacent carbon atoms, each one linking hydrogen atoms at opposite sides of the layer. Moreover,

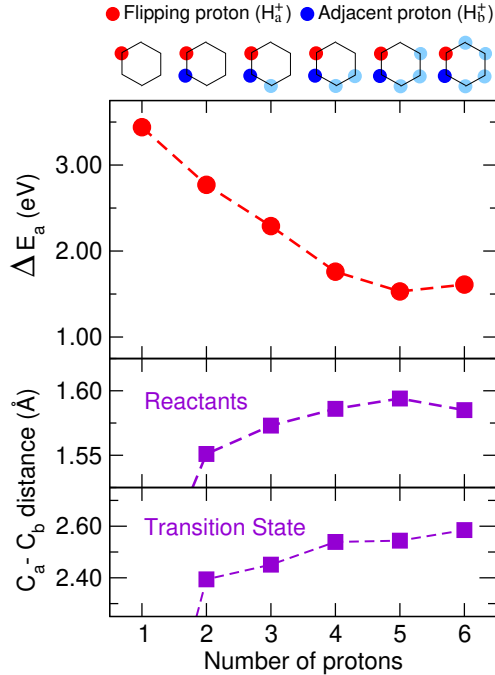


FIG. 4: Upper panel: Activation energy ΔE_a (in eV) for the permeation of a proton through a graphene prototype (circumcoronene) as a function of the number of chemisorbed protons along the central carbon ring. Initial configurations of the protons are schematically depicted in the upper part of the figure, where red and dark blue circles represent flipping (H_a^+) and adjacent (H_b^+) protons. Middle panel: distances between the corresponding carbon atoms C_a and C_b in the reactant state. Lower panel: same as middle panel for the transition state.

note that ΔE_r drops to about -1.20 eV for $n = 6$, indicating that the permeation process is globally more favorable when the graphenic ring protonation is complete. In this case a sp^3 configuration of the carbon atom bound to the flipped proton appears to be even more feasible as it is connected with two carbon atoms supporting protons on the other side, in an arrangement that is more similar to the typical chair conformation of graphane[31].

Interestingly, we have found that the permeation process exhibits different activation barriers and exothermicities depending on the position of the proton within a given row along a carbon ring. For instance, we have studied the case where the flipping proton is the central one in a row of five protons and compare the results with those of the $n = 5$

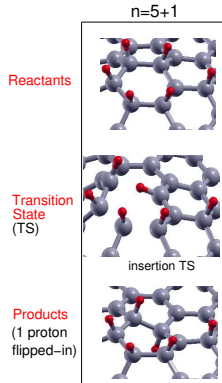


FIG. 5: Same as in Figs.2 and 3 for the case of five protons on a ring plus another one on a nearest neighbor ring.

case reported above, which shares the same reactant state but where the flipping proton is one at the end of the row (left panel of Fig. 3). The process occurs through the same kind of insertion TS but the activation energy is considerably larger (2.54 eV vs. 1.53 eV). We have noticed that at the TS the C_a-C_b distance is smaller than in the previous case; there are also some other differences in size, shape and flatness of the central and adjacent rings between the two TS being compared. In addition, exothermicity of this process is larger (-0.83 eV) than for the flipping of the external proton (-0.46 eV). As already discussed for $n=6$, the greater stability of the products can be related with a larger facility of the carbon atom linking the flipped proton to be arranged in a sp^3 geometry.

As can be foreseen from the previous results, it is a real challenge to identify the optimum configuration for the proton transport among a large number of different initial proton distributions. We have analyzed some more candidates and in Table I we show the obtained optimum configuration, named 5 + 1, corresponding to five protons adsorbed on the central ring plus another one on a nearest neighbor ring, as reported in Fig. 5. The related activation energy is only 1.0 eV which already can be considered consistent with the experimental determination[1], especially taking into account that a further reduction when

properly including tunneling effects could be expected. This brings strong support to the newly proposed mechanism which could provide a new perspective for the explanation of the experimental findings.

Moreover, we would also like to address the question of the reliability of present findings with respect to the size of the finite graphene prototype. To do that we have calculated the corresponding activation energy for the proton flipping process also for circumcircumcoronene ($C_{96}H_{24}$) whose estimations. Even if the energy barriers are globally larger for the larger prototype a similar trend can be observed in both cases: in fact, they decrease with the number of chemisorbed protons up to $n=5$ and, more importantly, reach a similar value around 1 eV for the $n=5+1$ case. These results suggest that low activation energies, which are compatible with the experimental findings, are expected also for larger graphene flakes.

Finally, there have been two previous theoretical studies which deserve special mention in connection with the present work, both of them already briefly mentioned in the Introduction. First we recall the work of Feng *et al*[14] where the importance of locally saturating carbon chemisorption sites via hydrogenation together with the associated change in carbon hybridization proved crucial in determining lower barriers for proton transport. We would like to stress some important differences with our proposed new mechanism. First, our model strictly includes the addition of protons as opposed to hydrogen atoms thus lending our approach closer to the proton permeation experimental conditions. Second and most important, the permeation process reported by Feng *et al* involves a completely different mechanism, as the proton is not initially chemisorbed (as in the present case) since the nearby chemisorbed sites are already saturated by hydrogenation, this unstability in the initial state leading to an important lowering of the barrier. Moreover, proton penetrates through the hole of the carbon ring, in contrast with the insertion transition state presented here. In this way, both mechanisms are qualitatively different, but with one not excluding the other.

The process reported here does bear a resemblance to the flip-in hydrogen insertion mechanism across a (5,5) SWCNT by Lee *et al*[21]. By means of periodic density-functional tight-binding calculations, they found a low energy path (with $\Delta E_a= 1.51$ eV) for hydrogen atom insertion into the middle of a very stretched C-C bond (detailed structure of the transition state not provided), a bond that is exothermically recovered after the hydrogen atom has flipped-in. These similarities were not necessarily foreseeable, given the differences

in the structure of the (very curved) (5,5) SWCNT and (flat) graphene and the well-known dependence of reactivity on the curvature of the carbon substrate[32]. However, they note that the flip-in process is efficient only if the nanotube is completely saturated, while an analogous conclusion for protonated graphene is not suggested from the present explorations. Also, the authors report even lower activation barriers for the subsequent flipping-in of nearby hydrogen atoms, a finding that is opposite to the test carried out with a second proton.

4. SUMMARY AND OUTLOOK

To summarize, we have reported DFT calculations of the permeation (flipping) of a proton through multiprotonated graphene, using circumcoronene as its molecular prototype. A new mechanism involving relatively low energy barriers (down to about 1.0 eV) has been found to occur when there is at least one other chemisorbed proton next to the flipping one. The corresponding transition state is characterized by the insertion of the proton into the middle of a C-C bond and a rearrangement of the hybridizations of the involved carbon atoms, with a recovering of that bond after the flipping is completed. The nature of this transition state as well as the enlargement of the C-C distances in the initial state is at the origin of the reduced activation energy as compared with the flipping of an isolated chemisorbed proton.

The lowest reported energy barrier is close to the experimentally measured activation energy (0.8 eV), and some contributions not taken into account in the present work -such as solvent effects[11–13], nuclear quantum effects[13–16, 33, 34] and bias potential[1, 2]- could actually play a role in further decreasing it. In the context of these experiments and within the frame of the adsorption-penetration model mentioned in the Introduction, it would be paramount to study the multiprotonation of graphene by proton transfer from the aqueous environment. A preliminary exploration indicates that the energy balance for the proton transfer from hydronium ions is strongly dependent on the size of the graphene prototype and that many effects such as the formation of adducts and the simulation of the aqueous medium should be carefully addressed. Moreover, we believe that it is worth to investigate whether related systems such as hydrogenated graphene or hydrogenated/protonated hexagonal boron nitride exhibit permeation processes with mechanisms analogous to that here reported. Work along some of these directions is in progress.

Acknowledgments

We gratefully thank N. Halberstadt and A. Beswick for valuable directions provided. We also thank Maciej Gutowski for many useful discussions on extended systems. The work has been funded by the Spanish grant FIS2017-84391-C2-2-P. Allocation of computing time by CESGA (Spain) is also acknowledged. RHL would like to thank CONACYT for a sabbatical scholarship.

- [1] S. Hu, M. Lozada-Hidalgo, F. C. Wang, A. Mishchenko, F. Schedin, R. R. Nair, E. W. Hill, D. W. Boukhvalov, M. I. Katsnelson, R. A. W. Dryfe, et al., *Nature* **516**, 227 (2014).
- [2] M. Lozada-Hidalgo, S. Hu, O. Marshall, A. Mishchenko, A. N. Grigorenko, R. A. W. Dryfe, B. Radha, I. V. Grigorieva, and A. K. Geim, *Science* **351**, 68 (2016).
- [3] V. Berry, *Carbon* **62**, 1 (2013).
- [4] M. Miao, M. B. Nardelli, Q. Wang, and Y. Liu, *Physical Chemistry Chemical Physics* **15**, 16132 (2013).
- [5] J. L. Achtyl, R. R. Unocic, L. Xu, Y. Cai, M. Raju, W. Zhang, R. L. Sacci, I. V. Vlassioug, P. F. Fulvio, P. Ganesh, et al., *Nature Communications* **6**, 6539 (2015).
- [6] M. I. Walker, P. Braeuninger-Weimer, R. S. Weatherup, S. Hofmann, and U. F. Keyser, *Applied Physics Letters* **107**, 213104 (2017).
- [7] X. Liu, Y. Gao, Y. Li, R. Wang, D. Zhu, Z. Xu, G. Ji, S. Jiang, B. Zhao, G. Yin, et al., *ACS Nano*. **11**, 8970 (2017).
- [8] M. Lozada-Hidalgo, S. Zhang, S. Hu, A. Esfandiar, I. V. Grigorieva, and A. K. Geim, *Nature Communications*. **8**, 15215 (2017).
- [9] S. Bukola, Y. Liang, C. Korzeniewski, J. Harris, and S. Creager, *Journal of the American Chemical Society* **140**, 1743 (2018).
- [10] M. Lozada-Hidalgo, S. Zhang, S. Hu, V. G. Kravets, F. J. Rodriguez, A. Berdyugin, A. Grigorenko, and A. K. Geim, *Nature Nanotechnology*. **13**, 300 (2018).
- [11] J. M. H. Kroes, A. Fasolino, and M. I. Katsnelson, *Phys. Chem. Chem. Phys.* **19**, 5813 (2017).
- [12] L. Shi, A. Xu, G. Chen, and T. Zhao, *The Journal of Physical Chemistry Letters*. **8**, 4354 (2017).

- [13] N. T. Ekanayake, J. Huang, J. Jakowski, B. G. Sumpter, and S. Garashchuk, *Journal of Physical Chemistry C* **121**, 24335 (2017).
- [14] Y. Feng, J. Chen, W. Fang, E.-G. Wang, A. Michaelides, and X.-Z. Li, *The Journal of Physical Chemistry Letters*. **8**, 6009 (2017).
- [15] I. Poltavsky, L. Zheng, M. Mortazavi, and A. Tkatchenko, *Journal of Chemical Physics* **148**, 204707 (2018).
- [16] J. W. Mazzuca and N. K. Haut, *Journal of Chemical Physics* **148**, 224301 (2018).
- [17] R. Balog, B. Jorgensen, L. Nilsson, M. Andersen, E. Rienks, M. Bianchi, M. Fanetti, E. Lsggaard, A. Baraldi, S. Lizzit, et al., *Nature Materials*. pp. 315–319 (2010).
- [18] M. Bonfanti, S. Achilli, and R. Martinazzo, *Journal of Physics. Condensed Matter* **30** (2018).
- [19] P. Merino, M. Svec, J. Martínez, P. Jelinek, P. Lacovig, M. Dalmiglio, S. Lizzit, P. Soukiassian, J. Cernicharo, and J. Martín-Gago, *Nature Communications*. **5** (2014).
- [20] J. I. Martínez, J. A. Martín-Gago, J. Cernicharo, and P. L. de Andres, *Journal of Physical Chemistry C* **118**, 26882 (2014).
- [21] S. M. Lee, K. H. An, G. Seifert, Y. H. Lee, and T. Frauenheim, *Journal of the American Chemical Society*. **123**, 5059 (2001).
- [22] M. Bartolomei, E. Carmona-Novillo, M. I. Hernández, J. Campos-Martínez, and F. Pirani, *J. Phys. Chem. C* **117**, 10512 (2013).
- [23] M. Bartolomei, R. P. de Tudela, K. Arteaga, T. González-Lezana, M. I. Hernández, J. Campos-Martínez, P. Villarreal, J. Hernández-Rojas, J. Bretón, and F. Pirani, *Phys. Chem. Chem. Phys.* **19**, 26358 (2017).
- [24] Y. Wang, H.-J. Qian, K. Morokuma, and S. Irle, *The Journal of Physical Chemistry A*. **116**, 7154 (2012).
- [25] E. Davidson, J. Klimes, D. Alfe, and A. Michaelides, *ACS Nano*. **8**, 9905 (2014).
- [26] J. Perdew, K. Burke, and M. Ernzerhof, *Phys. Rev. Lett.* **77**, 3865 (1996).
- [27] R. A. Kendall, T. H. Dunning, and R. J. Harrison, *J. Chem. Phys.* **96**, 6796 (1992).
- [28] J. S. Binkley, J. A. Pople, and W. J. Hehre, *J. Am. Chem. Soc.* **102**, 939 (1980).
- [29] M. J. Frisch, G. W. Trucks, H. B. Schlegel, G. E. Scuseria, M. A. Robb, J. R. Cheeseman, G. Scalmani, V. Barone, B. Mennucci, G. A. Petersson, et al., *Gaussian 09 Revision E.01*, gaussian Inc. Wallingford CT 2009.
- [30] R. Sumathy and E. S. Kryachko, *J. Phys. Chem. A* **106**, 510 (2002).

- [31] M. Pumera and C. H. A. Wong, *Chem. Soc. Rev.* **42**, 5987 (2013).
- [32] Z. Chen, W. Thiel, and A. Hirsch, *ChemPhysChem* **4**, 93 (2003).
- [33] M. I. Hernández, M. Bartolomei, and J. Campos-Martínez, *J. Phys. Chem. A* **119**, 10743 (2015).
- [34] A. Gijón, J. Campos-Martínez, and M. I. Hernández, *Journal of Physical Chemistry C*. **121**, 19751 (2017).